

Three-dimensional localization of the individual shallow NV center in diamond using a gold tip

Jiarui Qi^{1,2,3}, Xinghang Chen^{1,2,3}, Mengqi Wang^{1,2,3} ✉, and Ya Wang^{1,2,3,4} ✉

¹CAS Key Laboratory of Microscale Magnetic Resonance and School of Physical Sciences, University of Science and Technology of China, Hefei 230026, China;

²Anhui Province Key Laboratory of Scientific Instrument Development and Application, University of Science and Technology of China, Hefei 230026, China;

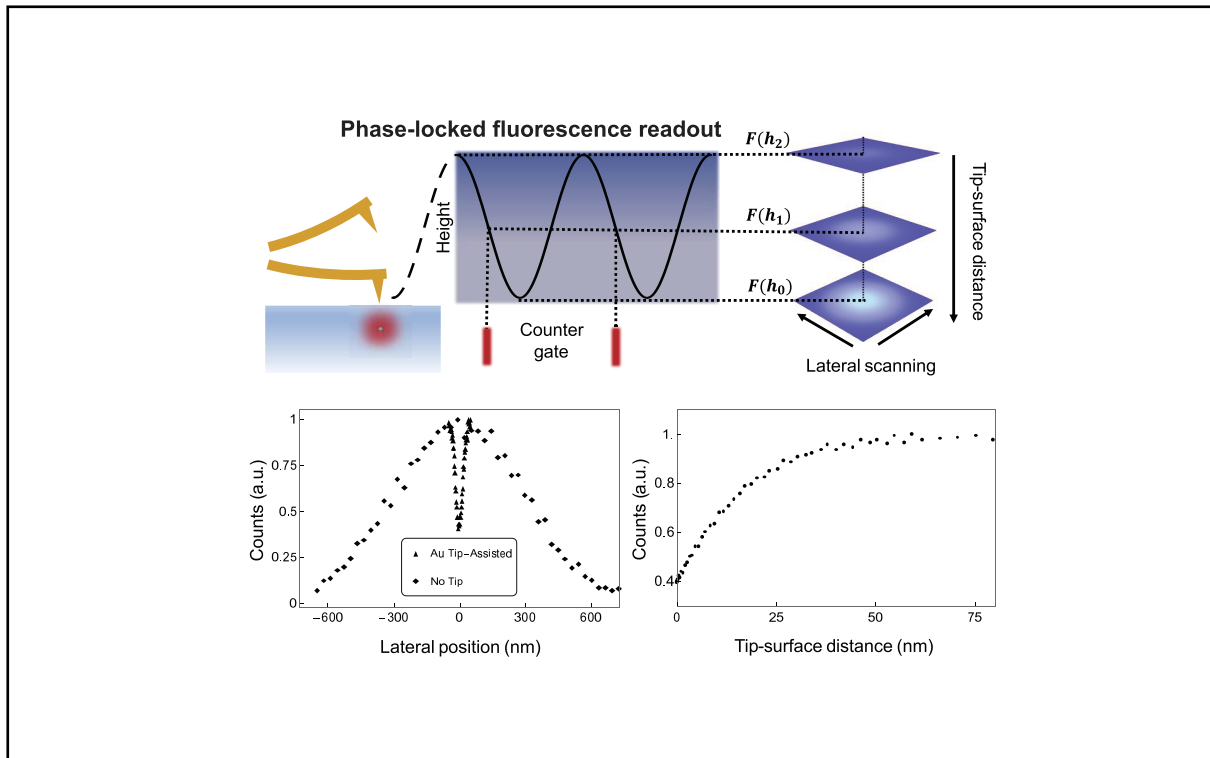
³CAS Center for Excellence in Quantum Information and Quantum Physics, University of Science and Technology of China, Hefei 230026, China;

⁴Hefei National Laboratory, University of Science and Technology of China, Hefei 230088, China

✉ Correspondence: Mengqi Wang, E-mail: mqw@ustc.edu.cn; Ya Wang, E-mail: ywustc@ustc.edu.cn

© 2025 The Author(s). This is an open access article under the CC BY-NC-ND 4.0 license (<http://creativecommons.org/licenses/by-nc-nd/4.0/>).

Graphical abstract



The near-field effect between a gold tip and the NV center can be used for 3D localization of individual NV center.

Public summary

- In this study, we use the near-field quenching effect of the tip to achieve three-dimensional super-resolution localization of the near-surface NV center.
- The super-resolution technique based on near-field quenching has the advantages of real-space imaging, fast imaging speed, and three-dimensional super-resolution.
- This approach can easily be combined with nanomechanical or electrical operations on NV centers.

Three-dimensional localization of the individual shallow NV center in diamond using a gold tip

Jiarui Qi^{1,2,3}, Xinghang Chen^{1,2,3}, Mengqi Wang^{1,2,3} ✉, and Ya Wang^{1,2,3,4} ✉

¹CAS Key Laboratory of Microscale Magnetic Resonance and School of Physical Sciences, University of Science and Technology of China, Hefei 230026, China;

²Anhui Province Key Laboratory of Scientific Instrument Development and Application, University of Science and Technology of China, Hefei 230026, China;

³CAS Center for Excellence in Quantum Information and Quantum Physics, University of Science and Technology of China, Hefei 230026, China;

⁴Hefei National Laboratory, University of Science and Technology of China, Hefei 230088, China

✉ Correspondence: Mengqi Wang, E-mail: mqw@ustc.edu.cn; Ya Wang, E-mail: ywustc@ustc.edu.cn

© 2025 The Author(s). This is an open access article under the CC BY-NC-ND 4.0 license (<http://creativecommons.org/licenses/by-nc-nd/4.0/>).



Cite This: *JUSTC*, 2025, 55(4): 0404 (5pp)



Read Online

Abstract: This work presents a method for the three-dimensional localization of individual shallow NV center in diamond, leveraging the near-field quenching effect of a gold tip. Our experimental setup involves the use of an atomic force microscope to precisely move the gold tip close to the NV center, while simultaneously employing a home-made confocal microscope to monitor the fluorescence of the NV center. This approach allows for lateral super-resolution, achieving a full width at half maximum (FWHM) of 38.0 nm and a location uncertainty of 0.7 nm. Additionally, we show the potential of this method for determining the depth of the NV centers. We also attempt to determine the depth of the NV centers in combination with finite-difference time-domain (FDTD) simulations. Compared to other depth determination methods, this approach allows for simultaneous lateral and longitudinal localization of individual NV centers, and holds promise for facilitating manipulation of the local environment surrounding the NV center.

Keywords: NV center; super-resolution localization; atom force microscopy

CLC number: O4-34

Document code: A

1 Introduction

The nitrogen-vacancy (NV) center in diamond has been widely applied in quantum sensing, such as electric and magnetic field imaging and sensing^[1-3], stress and temperature detection^[4-6], and quantum information processing^[7,8]. In these applications, achieving three-dimensional localization of the NV center at the nanoscale is a crucial requirement. And many efforts have been devoted to the localization of NV centers, such as super-resolution optical imaging^[9-12], magnetic resonance detection under a gradient magnetic field^[13-15], and near-field optical imaging assisted by atomic force microscopy (AFM)^[16,17].

Among these methods, techniques based on AFM assistance can accurately obtain NV center position information using the diamond morphology as a reference, which is conducive to further experimental research on the diamond surface. In our previous work, we demonstrated the two-dimensional localization of the NV center in the diamond with nanometer precision using an atomic force microscopy combined confocal optical system^[16]. However, the localization of the individual NV center in the depth direction based on AFM has not been achieved yet.

Methods for determining the depth of NV centers, such as the NMR technique, have limitations in the very shallow

individual NV center due to the instability of their optical and/or spin properties^[18]. As for the FRET technique, this method requires using the NV center as a scanning probe, with specific requirements for the sample and usage scenario^[19]. In conclusion, near-field tip-assisted technique can be an easy way to determine the position of the individual shallow NV center precisely, which is useful for quantum applications of NV center^[20-22].

In this study, we present a method for the three-dimensional localization of the near-surface NV center in diamond, based on the near-field quenching effect of a gold tip. Utilizing the sensitivity of NV center fluorescence quenching efficiency to distances from the tip, depth localization can be achieved. Through the finite-difference time-domain (FDTD) simulations, we establish a correlation between quenching efficiency and tip distance. And by characterizing the quenching efficiency under tip interaction, we analyze of NV center depths statistically.

2 Experiment setup and protocols

As shown in Fig. 1a, the near-field effect of a metal nanoparticle can significantly quench a fluorescent molecule, and the quenching efficiency is very sensitive to distance within a few tens of nanometers. We can utilize the sensitivity of the

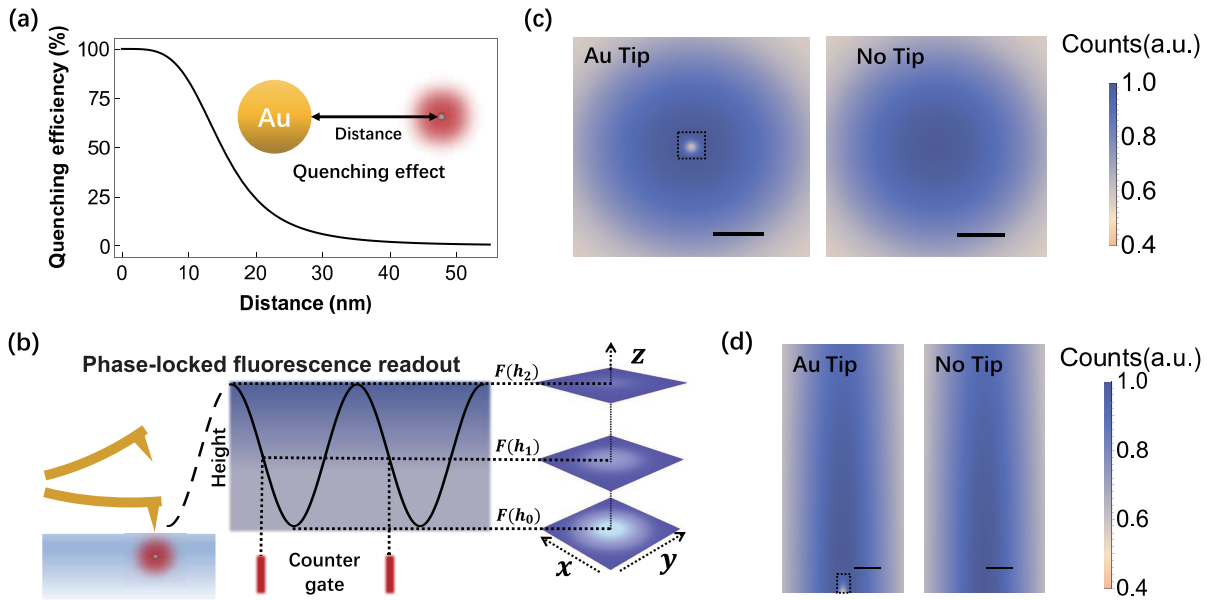


Fig. 1. Experimental theory and setup diagrams. (a) Quenching efficiency of a metal nanoparticle for a fluorescent molecule. Reproduced with permission from Ref. [23]. Copyright 2013, American Chemical Society. (b) Schematic diagram of the experimental setup. The left part shows an AFM cantilever (yellow) shaking above an NV center (red) in diamond (light blue); the middle part shows the phase-locked fluorescence readout process; the right part shows the fluorescence image obtained by scanning the sample stage at different tip heights. (c) Schematic diagram of the lateral fluorescence image of an individual NV center with and without a near-field gold tip. The dashed box in the left image corresponds to the two-dimensional fluorescence image at h_0 in (b). (d) Schematic diagram of the longitudinal section of the NV center fluorescence with and without a gold tip. The dashed box on the left corresponds to the central point ($x = 0$) of the fluorescence image from h_0 to h_2 in (b). The scale bars in (c) and (d) represent 100 nm.

near-field quenching effect of a gold tip to locate the individual NV center precisely.

According to the principles described above, we construct an AFM-confocal platform refer to previous work^[16]. The AFM is used to manipulate a gold tip approaching to the NV center, and the home-built confocal microscope is employed to monitor the fluorescence intensity. In this experiment, the AFM works in the tapping mode, and the oscillation of the cantilever is sinusoidal. As shown in Fig. 1b, to selectively collect fluorescence from NV centers at different tip heights, we employ the phase-locked fluorescence readout technique. This method utilizes periodic square-wave pulses synchronized with the probe vibration as a counter gate to control the fluorescence readout. By adjusting the relative phase between the square-wave pulse and the probe vibration, we can capture the fluorescence response from NV centers at varying tip heights. The width of the square-wave pulse defines the time window for fluorescence collection, and in this experiment, we choose a readout window size of 1/10 of the probe vibration period. Combined with the AFM sample scanner, we can collect the fluorescence of the NV center when the tip is at any relative tip-NV center position. Fig. 1c and d shows a comparative illustration of the resolution of the NV center with and without a gold tip.

In this experiment, we utilize the diamond chip whose surface is etched to form the nano-pillar to improve fluorescence collection efficiency. Nitrogen ions are selectively implanted into each nano-pillar to create NV centers by self-aligned technique^[24]. Here, we chose a commercial gold-coated probe (PPP-NCHAu-10, NanoSensor) for the experiment, which is the common metal-coated probe. The cantilever oscillation amplitude is 57.3 nm, and the frequency is 270.5 kHz.

3 Experiment results

Based on the setup shown in Fig. 1b, we try the lateral super-resolution and depth determination experiment. The objective lens is pre-aligned refer to the previous work^[16]. During the lateral experiment, we tuned the counter gate to count at the closest tip-surface distance, and the AFM sample stage is scanning. During the depth determination experiment, we use the lateral super-resolution result to move the AFM scanner, aiming to align tip and NV center laterally.

Firstly, we achieve the lateral super-resolution for the NV center. Fig. 2a shows the lateral super-resolution image of an individual NV center using a gold tip. Compared with the non-tip confocal image with an FWHM of 701 nm and a location uncertainty of 6 nm, the gold tip-assisted image shows superior performance. The super-resolution image assisted by the Au tip achieves an FWHM of 38.0 nm and a location uncertainty of 0.7 nm, as depicted in Fig. 2c.

According to the lateral super-resolution results, we can position the tip precisely above the NV center with nanometer accuracy. Then we can try depth localization of the NV center. Fig. 3a shows the fluorescence counts of the NV center versus the tip-surface distance when the tip is exactly above the NV center. Here, we use quenching efficiency $E_{Dis} = 1 - F_{Tip}/F_0$ to serve as a parameter for characterizing quenching capability^[25], where F_{Tip} is the fluorescence counts of NV center with a near-field gold tip, F_0 is the reference fluorescence counts of NV center without a gold tip. Fig. 3a shows that the quenching efficiency of the NV center is highly dependent on the tip-surface distance when it is less than 50 nm, which can be used for precise depth determination of the shallow NV center.

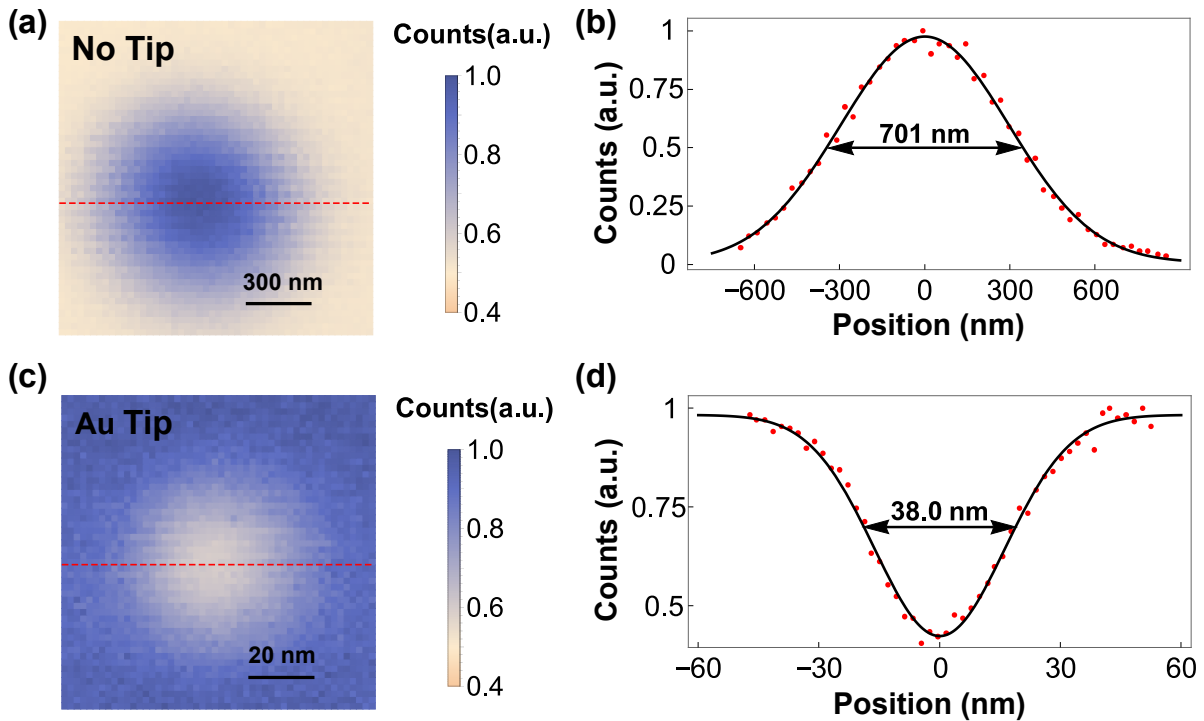


Fig. 2. Lateral super-resolution imaging based on the near-field quenching effect of the gold tip. (a) Two-dimensional confocal fluorescence image of an individual NV center without a gold tip. (b) Line profile along the red line in (a). The red dots represent the experimental fluorescence counts, and the black solid line is the corresponding Gaussian fitting curve. (c) Two-dimensional confocal fluorescence image of the NV center with a gold tip. (d) Line profile along the red line in (c). The red dots represent the experimental fluorescence counts, and the black solid line is the corresponding Gaussian fitting curve. The counts of (b) and (d) can be expressed as $F(r) = Ae^{-(r-r_0)^2/2\sigma^2} + C$. r is the lateral position, and $F(r)$ is the corresponding counts. r_0 , A , C , and σ are fitting parameters, and $\text{FWHM} = 2\sqrt{2\ln 2}\sigma$. The location uncertainty is double the standard deviation of the fitting estimate r_0 ($k=2$, 95% confidence interval).

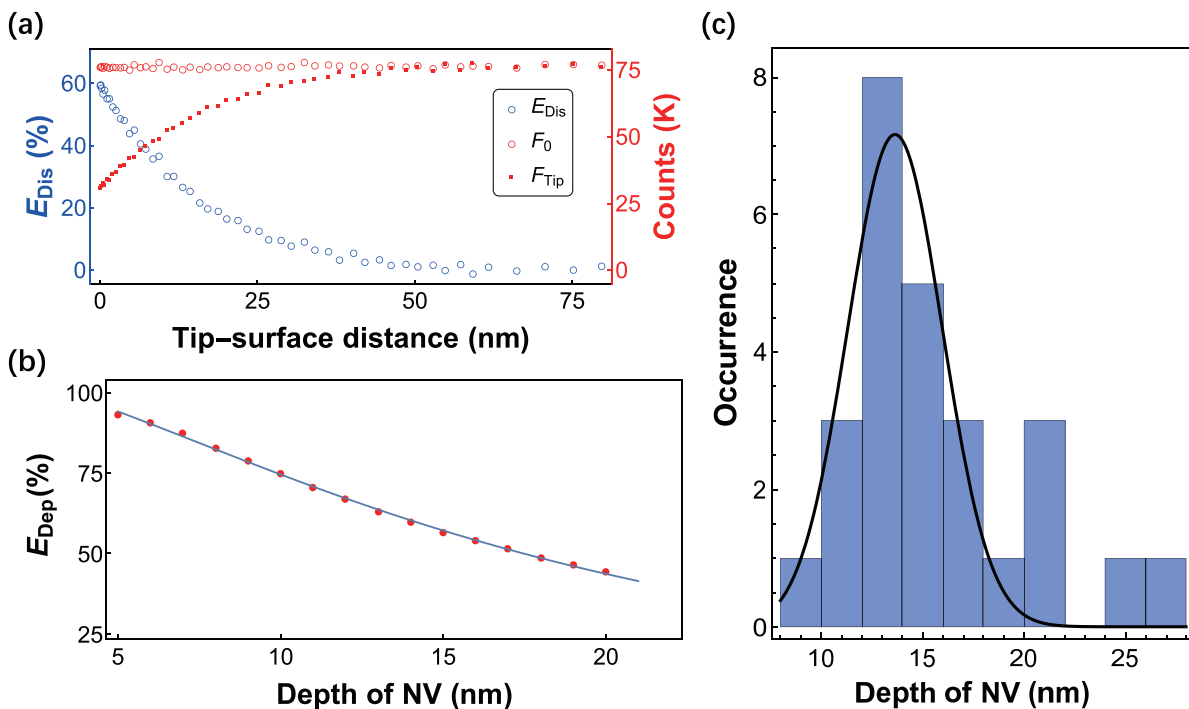


Fig. 3. Depth determination for NV center based on the quenching effect of the gold tip. (a) Fluorescence and contrast of an individual NV center versus the tip-surface distance (experimental result). (b) The quenching efficiency as a function of the NV center depth when the tip is closest to the surface (simulated result). The red solid dots represent the results obtained from FDTD simulations; the blue solid line represents the quantitative relationship obtained by fitting using Eq. (1); the fitted result is $E_{\text{Dep}} = 1/(0.914 + 0.017d_{\text{NV}} + 0.0026d_{\text{NV}}^2)$. (c) Histogram of the depth distribution of 26 NV centers obtained from experiment results. The black solid line is the corresponding Gaussian fitting curve.

To determine the depth of the NV center, we use the FDTD simulation to build the relationship between the quenching efficiency and the depth of the NV center when the tip touches the diamond surface above the NV center. In the simulation, the tip-surface distance is 2 nm, considering the surface roughness of the diamond and the average distance in the readout window. The quenching efficiency E_{Dep} is monitored with various depths of the NV center in simulations. The simulation results are depicted in Fig. 3b, and the relationship between the quenching efficiency and the depth of the NV center is numerically simplified to the expression:

$$E_{\text{Dep}} = \frac{1}{a_0 + a_1 d_{\text{NV}} + a_2 d_{\text{NV}}^2}, \quad (1)$$

where a_0, a_1, a_2 are fitting parameters, and d_{NV} is the depth of NV center. Thus, we give a quantitative formula to describe the relationship between E_{Dep} and d_{NV} . The depth of the NV in Fig. 3a is $14.1 \text{ nm} \pm 0.2 \text{ nm}$ with a quenching efficiency of 60.0% when the tip touches the diamond surface.

Finally, we measure the depth of 26 individual NV centers using a gold tip to check the reliability of this method. Fig. 4c shows the histogram of the depth of NV centers obtained from the experiment. It shows that under 15 keV $^{15}\text{N}_2^+$ ion implantation, the generation of NV centers has a distribution with a center depth of 13.7 nm and an FWHM of 5.5 nm. The stopping and range of ions in matter (SRIM) Monte-Carlo simulation of $^{15}\text{N}_2^+$ implanted into diamond with a kinetic energy of 15 keV predicts that the distribution of nitrogen atoms has a projected range of 11 nm and a longitudinal straggling of 4.1 nm. The depth of individual NV centers is slightly larger than SRIM simulation probably because SRIM does not take crystallographic effects such as ion channeling into consideration^[18,21,26].

4 Discussion

In this section, we will discuss two main issues that arise during the experiment.

First, the state of the tip changes during scanning; this will affect the quenching efficiency and thus the accuracy of depth determination. As shown in Fig. 4a–c, after a long time experiment, the quenching efficiency for the same NV center decreased from 56.2% to 24.7%. To ensure the reliability of the experimental results, we need to improve the experimental procedure to maintain the integrity and cleanliness of the tip. Or, we can use a standard sample to calibrate the coefficients in Eq. (1) in advance.

Second, we chose a gold tip instead of a silicon tip for our three-dimensional super-resolution localization experiments. Previous studies utilized silicon as the tip material for achieving high resolution^[6]. However, as depicted in Fig. 4d–f, we observed that the quenching effect of the silicon tip is inferior to that of the gold tip. To obtain a better signal-to-noise ratio, we chose to use a gold tip for super-resolution localization of NV centers.

5 Conclusions

In this work, we present a new method to determine the three-dimensional location of the shallow individual NV center using a gold tip based on the near-field quenching effect. First, we achieve lateral super-resolution with an FWHM of 38.0 nm and a location uncertainty of 0.7 nm. Compared with a silicon tip, a gold tip is advantageous for lateral positioning. Then we demonstrate the depth determination of the shallow NV center based on the high sensitivity of the near-field effect. The results show that the generation of NV center has a center depth of 13.7 nm and an FWHM of 5.5 nm.

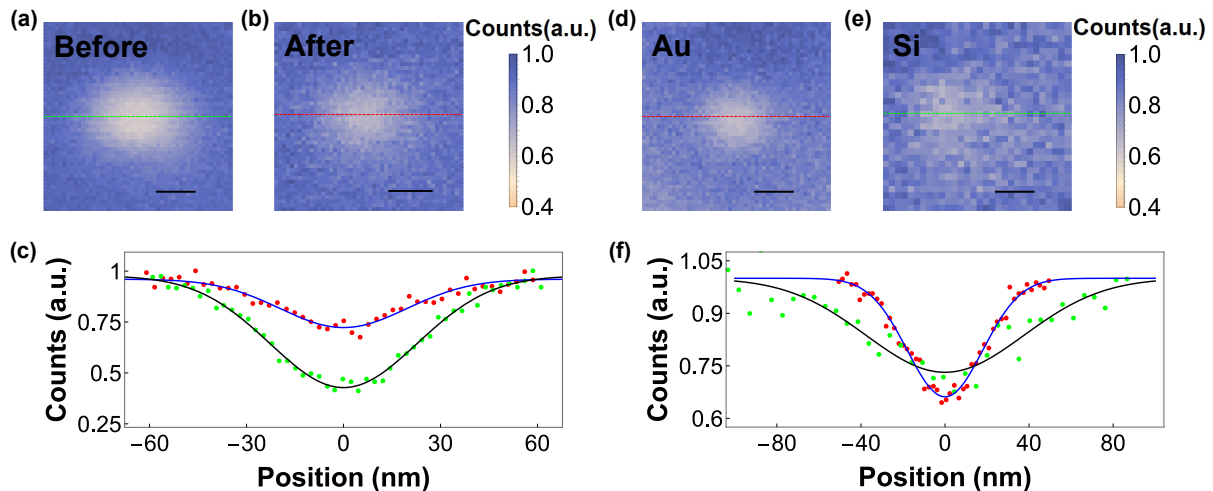


Fig. 4. The impact of the tip condition and material on super-resolution performance. (a) Lateral super-resolution image of the NV center before a long-term experiment. Scale bar: 24 nm. (b) Lateral super-resolution image of the same NV center with (a) after long-term experiment. Scale bar: 24 nm. (c) Comparison of lateral super-resolution results of the same NV center before and after long-term experiment. Green solid points and black solid line represent fluorescence counts along the green line in (a) and the corresponding Gaussian fitting curve; red solid points and the blue solid line represent fluorescence counts along the green line in (b) and the corresponding Gaussian fitting curve. (d) Lateral super-resolution image of the NV center assisted by a gold tip. Scale bar: 20 nm. (e) Lateral super-resolution image of the same NV center with (d) assisted by a silicon tip. Scale bar: 40 nm. (f) Comparison of lateral super-resolution results of the NV center assisted by different tips. Green solid points and black solid line represent fluorescence counts along the green line in (e) and the corresponding Gaussian fitting curve; red solid points and the blue solid line represent fluorescence counts along the green line in (d) and the corresponding Gaussian fitting curve.

Acknowledgements

This work was supported by the National Natural Science Foundation of China (T2325023, 92265204, 12104447), the National Key R&D Program of China (2023YFF0718400), the Innovation Program for Quantum Science and Technology (2021ZD0302200), and the Fundamental Research Funds for the Central Universities.

Conflict of interest

The authors declare that they have no conflict of interest.

Biographies

Jiarui Qi is a master student at the University of Science and Technology of China. She received her Bachelor's degree from Jilin University in 2021. Her research mainly focuses on the nanoscale manipulation of NV centers using atomic force microscopy.

Mengqi Wang is currently an Associate Researcher at the University of Science and Technology of China (USTC). He received his Ph.D. degree from USTC in 2019. His research mainly focuses on the fabrication and application of diamond-based quantum sensors.

Ya Wang is currently a Professor at the University of Science and Technology of China (USTC). He received his Ph.D. degree from USTC in 2012. His research mainly focuses on the fabrication, spin control, and application technology development of high-performance diamond quantum devices.

References

- [1] Bian K, Zheng W, Zeng X, et al. Nanoscale electric-field imaging based on a quantum sensor and its charge-state control under ambient condition. *Nature Communications*, **2021**, *12*: 2457.
- [2] Huxter W S, Sarott M F, Trassin M, et al. Imaging ferroelectric domains with a single-spin scanning quantum sensor. *Nature Physics*, **2023**: 644–648.
- [3] Sun Q C, Song T, Anderson E, et al. Magnetic domains and domain wall pinning in atomically thin CrBr₃ revealed by nanoscale imaging. *Nature Communications*, **2021**, *12*: 1989.
- [4] Doherty M W, Struzhkin V V, Simpson D A, et al. Electronic properties and metrology applications of the diamond NV⁻ center under pressure. *Physical Review Letters*, **2014**, *112*: 047601.
- [5] Acosta V M, Bauch E, Ledbetter M P, et al. Temperature dependence of the nitrogen-vacancy magnetic resonance in diamond. *Physical Review Letters*, **2010**, *104*: 070801.
- [6] Kucsko G, Maurer P C, Yao N Y, et al. Nanometre-scale thermometry in a living cell. *Nature*, **2013**, *500*: 54–58.
- [7] Van der Sar T, Wang Z H, Blok M S, et al. Decoherence-protected quantum gates for a hybrid solid-state spin register. *Nature*, **2012**, *484*: 82–86.
- [8] Xu K, Xie T, Li Z, et al. Experimental adiabatic quantum factorization under ambient conditions based on a solid-state single spin system. *Physical Review Letters*, **2017**, *118*: 130504.
- [9] Rittweger E, Han K Y, Irvine S E, et al. STED microscopy reveals crystal colour centres with nanometric resolution. *Nature Photonics*, **2009**, *3* (3): 144–147.
- [10] Pfender M, Aslam N, Waldherr G, et al. Single-spin stochastic optical reconstruction microscopy. *Proceedings of the National Academy of Sciences of the United States of America*, **2014**, *111*: 14669–14674.
- [11] Chen X, Zou C, Gong Z, et al. Subdiffraction optical manipulation of the charge state of nitrogen vacancy center in diamond. *Light: Science & Applications*, **2015**, *4*: e230.
- [12] Castelletto S, Boretti A. Color centers in wide-bandgap semiconductors for subdiffraction imaging: A review. *Advanced Photonics*, **2021**, *3*: 054001.
- [13] Arai K, Belthangady C, Zhang H, et al. Fourier magnetic imaging with nanoscale resolution and compressed sensing speed-up using electronic spins in diamond. *Nature Nanotechnology*, **2015**, *10*: 859–864.
- [14] Grinolds M S, Maletinsky P, Hong S, et al. Quantum control of proximal spins using nanoscale magnetic resonance imaging. *Nature Physics*, **2011**, *7*: 687–692.
- [15] Huang Y, Guo M, Shen M, et al. Superresolution localization of nitrogen-vacancy centers in diamond with quantum-controlled photoswitching. *Physical Review A*, **2020**, *102* (4): 040601.
- [16] Ye X, Wang M, Wang P, et al. Nanoscale localization of the near-surface nitrogen vacancy center assisted by a silicon atomic force microscopy probe. *Journal of Physics: Photonics*, **2021**, *3*: 014003.
- [17] Hui Y, Lu Y C, Su L J, et al. Tip-enhanced sub-diffraction fluorescence imaging of nitrogen-vacancy centers in nanodiamonds. *Applied Physics Letters*, **2013**, *102*: 013102.
- [18] Pham L M, DeVience S J, Casola F, et al. NMR technique for determining the depth of shallow nitrogen-vacancy centers in diamond. *Physical Review B*, **2016**, *93*: 045425.
- [19] Tisler J, Oeckinghaus T, Stöhr R J, et al. Single defect center scanning near-field optical microscopy on graphene. *Nano Letters*, **2013**, *13*: 3152–3156.
- [20] Ishizu S, Sasaki K, Misonou D, et al. Spin coherence and depths of single nitrogen-vacancy centers created by ion implantation into diamond via screening masks. *Journal of Applied Physics*, **2020**, *127*: 244502.
- [21] Haque A, Sumaiya S. An overview on the formation and processing of nitrogen-vacancy photonic centers in diamond by ion implantation. *Journal of Manufacturing and Materials Processing*, **2017**, *1*: 6.
- [22] Wang J, Zhang W, Zhang J, et al. Coherence times of precise depth controlled NV centers in diamond. *Nanoscale*, **2016**, *8*: 5780–5785.
- [23] Breshike C J, Riskowski R A, Strouse G F. Leaving Förster resonance energy transfer behind: Nanometal surface energy transfer predicts the size-enhanced energy coupling between a metal nanoparticle and an emitting dipole. *The Journal of Physical Chemistry C*, **2013**, *117*: 23942–23949.
- [24] Wang M, Sun H, Ye X, et al. Self-aligned patterning technique for fabricating high-performance diamond sensor arrays with nanoscale precision. *Science Advances*, **2022**, *8* (38): eabn9573.
- [25] Yun C S, Javier A, Jennings T, et al. Nanometal surface energy transfer in optical rulers, breaking the FRET barrier. *Journal of the American Chemical Society*, **2005**, *127*: 3115–3119.
- [26] Toyli D M, Weis C D, Fuchs G D, et al. Chip-scale nanofabrication of single spins and spin arrays in diamond. *Nano Letters*, **2010**, *10* (8): 3168–3172.